Introduction to Organic Electronic and Optoelectronic Materials and Devices 2nd edition Sun Solutions Manual

SKU: 9781466585102-SOLUTIONS

Chapter 2 Introduction to Optoelectronic Device Principles

Joachim Piprek
NUSOD Institute, Newark, DE 19714-7204
Email: piprek@ieee.org

QUESTION 1: A solar cell under illumination of 500 W/m^2 has a short circuit current of I_{sc} = 15 mA and an open circuit voltage of V_{oc} = 0.6 V. Calculate I_{sc} and V_{oc} for double the light intensity assuming a diode ideality factor of $m=1$.

SOLUTION 1: The solar cell current-voltage characteristic is given by Eq. (12). The open circuit voltage is obtained for $I=0$ and $V_{oc} >> mkT/e$ as

$$V_{oc} = \frac{mkT}{e} \ln\left(\frac{I_{ph}}{I_o}\right)$$

The short circuit current is equal to the photocurrent which is proportional to the light intensity. Double the intensity gives I_{sc2} = 30 mA and

$$V_{oc2} = V_{oc1} + \frac{mkT}{e} \ln\left(\frac{I_{sc2}}{I_{sc1}}\right) = 0.6V + 0.0259V \times \ln(2) = 0.618V \ .$$

QUESTION 2: The LED emission wavelength λ is sensitive to the temperature T which is mainly related to the band gap shift $E_g(T)$. Consider an LED with an emission wavelength of 870 nm at 20 ^{o}C that red-shifts by 2.8 nm for 10 ^{o}C temperature increase. What is the band gap E_g and its temperature sensitivity $\Delta E_g/\Delta T$?

SOLUTION 2: The band gap – wavelength relation is given in Eq. (1). At 20

^{o}C, the wavelength of 870 nm gives a band gap of $E_g = 1241/870 = 1.426$ eV. The thermal shift of the band gap is calculated as

$$\frac{\Delta E_g}{\Delta T} = \frac{1241}{10}\left(\frac{1}{870} - \frac{1}{867.2}\right) = -0.46 \times 10^{-3}\,\frac{eV}{K}\,.$$

QUESTION 3: Consider a Mach-Zehnder modulator as in Figure 23 with a Pockels coefficient $r = 3.4\ 10^{-12}$ m/V and a branch thickness $d = 5$ µm. For a maximum half-wave voltage of $V_\pi = 10$ V, what should be the minimum branch length L for modulator operation at 1.55 µm wavelength ($n_r = 2.2$) ?

SOLUTION 3: The half-wave voltage is given by Eq. (35), which leads to

$$L = \frac{d}{V_\pi}\frac{\lambda}{rn_r^3} = \frac{5\times10^{-6}m}{10V}\frac{1.55\times10^{-6}m}{3.4\times10^{-12}m/V\times2.2^3} = 2.14cm\,.$$

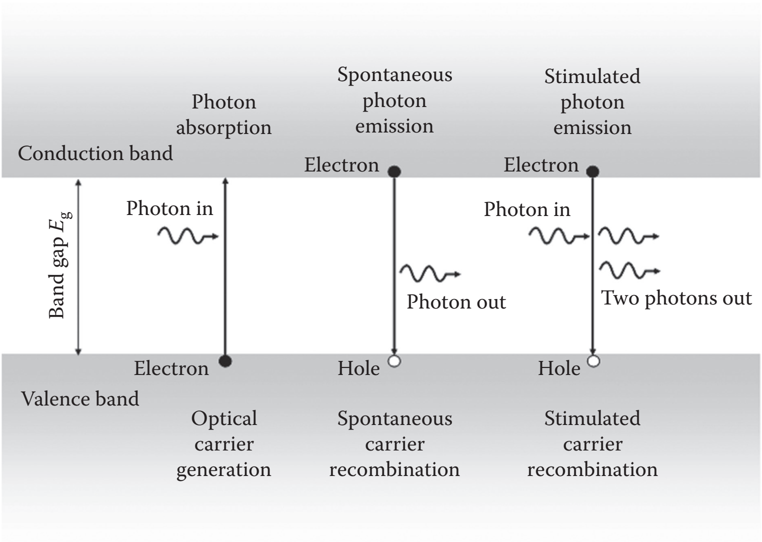

Figure 2.1 Illustration of key processes in optoelectronic devices.

002x001.eps

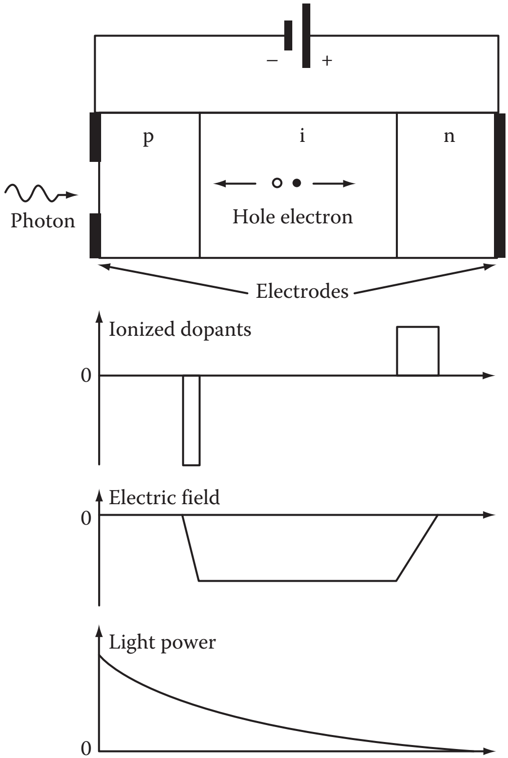

Figure 2.2 Schematic structure and internal physics of pin photodiodes.

002x002.eps

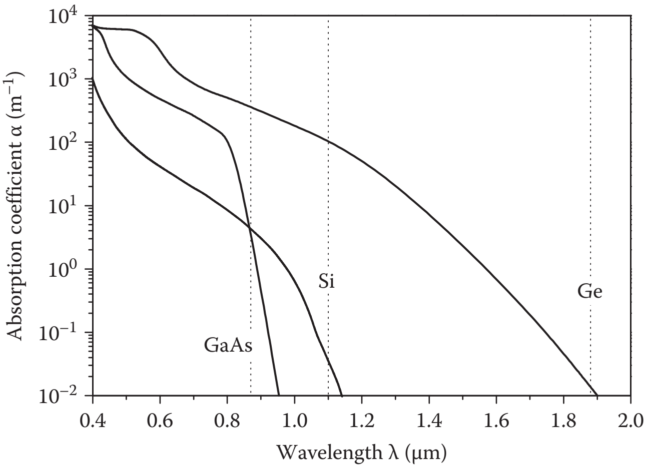

Figure 2.3 Optical absorption constants of GaAs, Si, and Ge as function of light wavelength. The dotted lines indicate the band gap wavelength.

002x003.eps

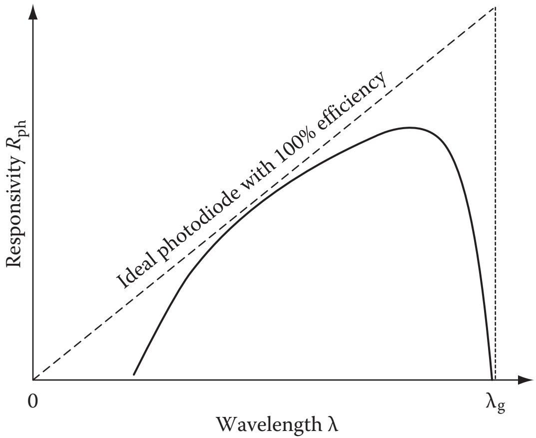

Figure 2.4 Schematic responsivity spectrum of photodiodes.

002x004.eps

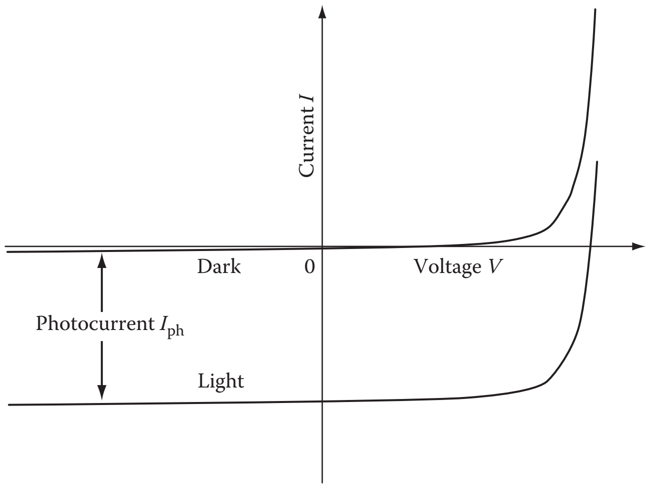

Figure 2.5 Current–voltage characteristic for a photodiode with and without illumination.

002x005.eps

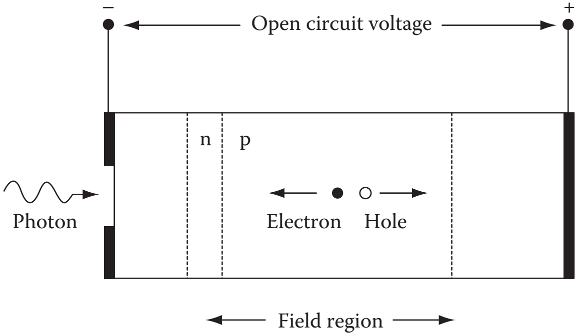

Figure 2.6 Solar cell.

002x006.eps

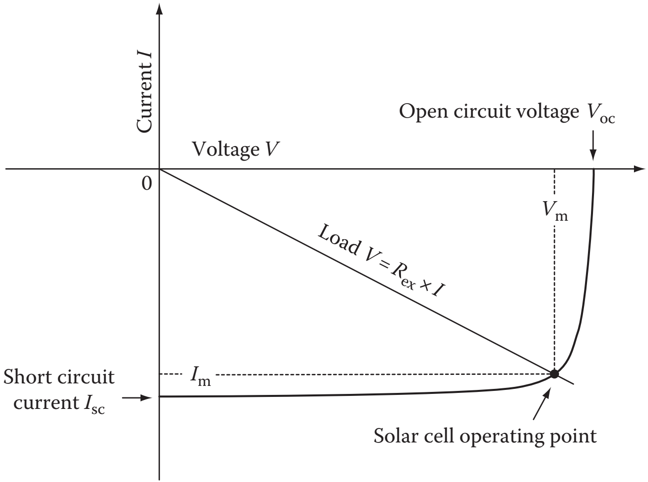

Figure 2.7 Solar cell current–voltage characteristic and parameters.

002x007.eps

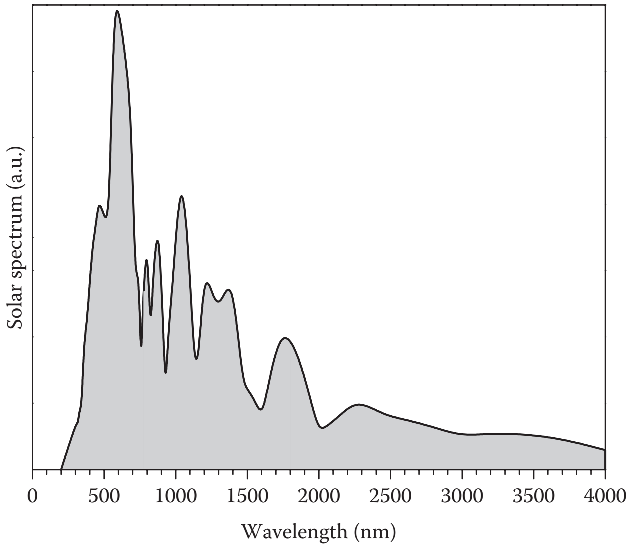

Figure 2.8 Solar spectrum.

002x008.eps

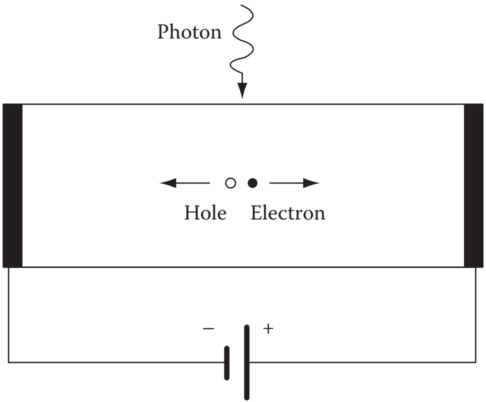

Figure 2.9 Photoconductor.

002x009.eps

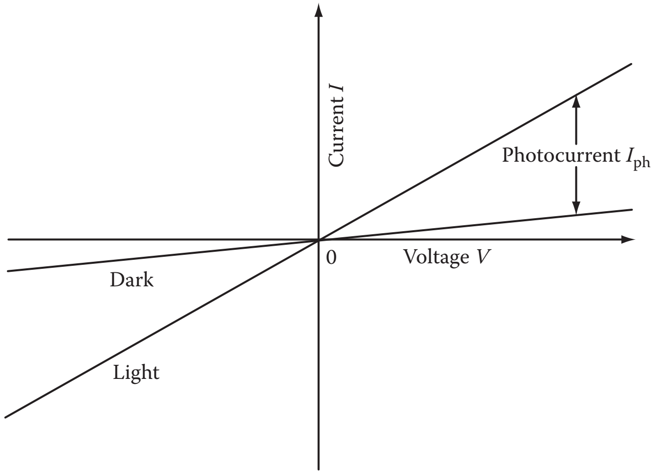

Figure 2.10 Current–voltage characteristic for a photoconductor with and without illumination.

002x010.eps

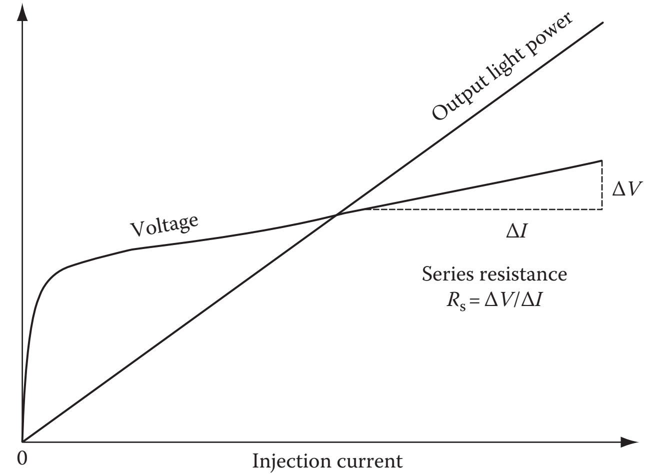

Figure 2.11 Typical LED characteristics: light versus current (*LI*) and voltage versus current (*IV*).

002x011.eps

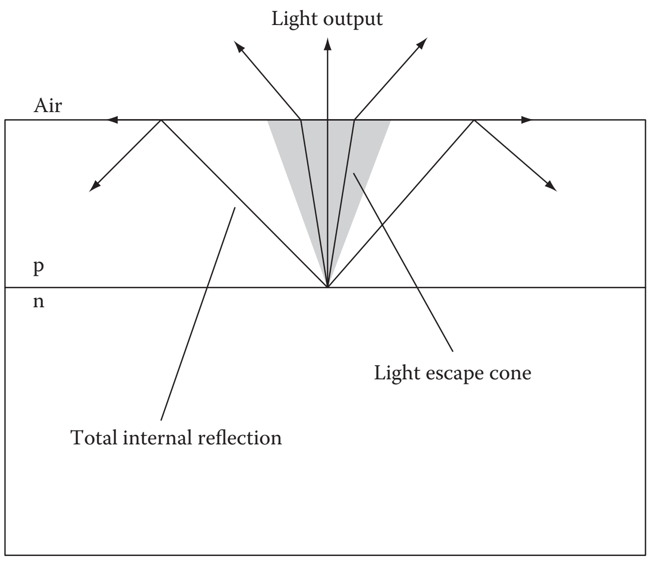

Figure 2.12 Illustration of light propagation in a simple LED structure.

002x012.eps

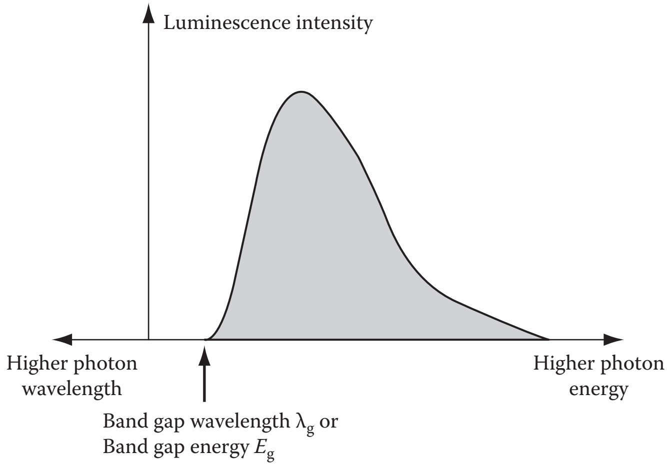

Figure 2.13 Schematic LED emission spectrum.

002x013.eps

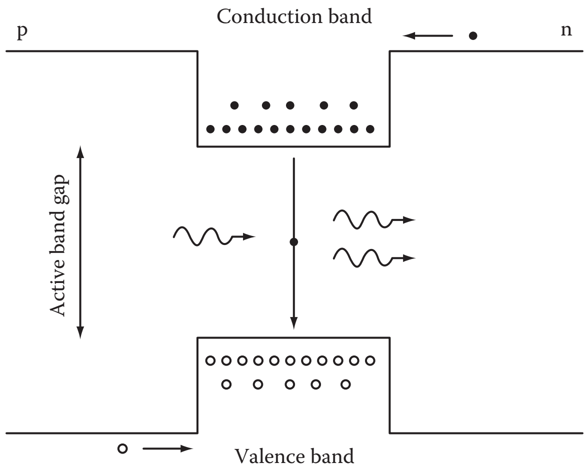

Figure 2.14 Energy band diagram of a pin heterojunction illustrating stimulated photon emission at forward bias.

002x014.eps

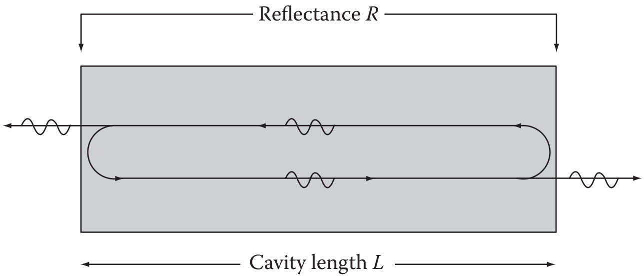

Figure 2.15 Optical feedback in a Fabry–Perot laser.

002x015.eps

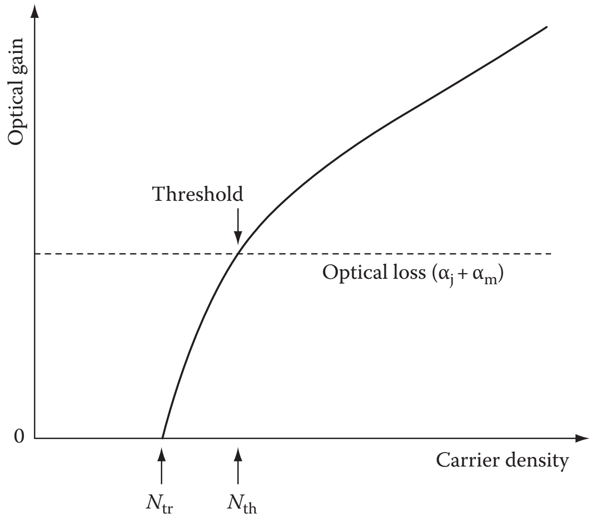

Figure 2.16 Gain versus carrier density $g(N)$ with transparency density N_{tr} and threshold density N_{th}.

002x016.eps

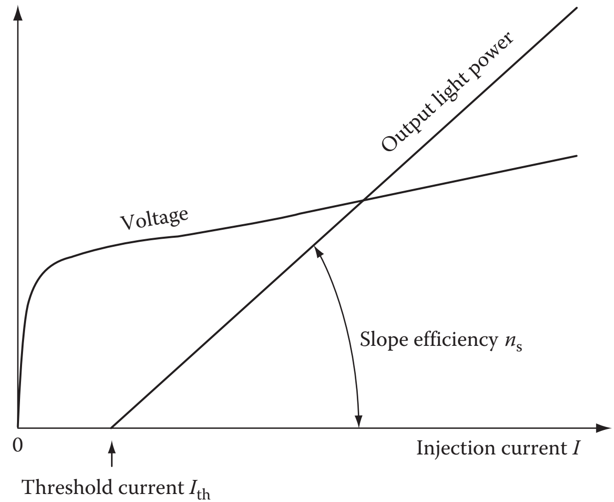

Figure 2.17 Laser characteristics: light power versus current (*LI*) and voltage versus current (*IV*).

002x017.eps

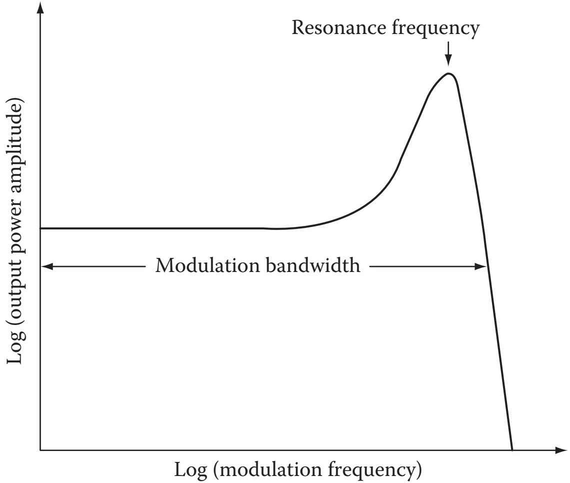

Figure 2.18 Analog modulation characteristic of a laser.

002x018.eps

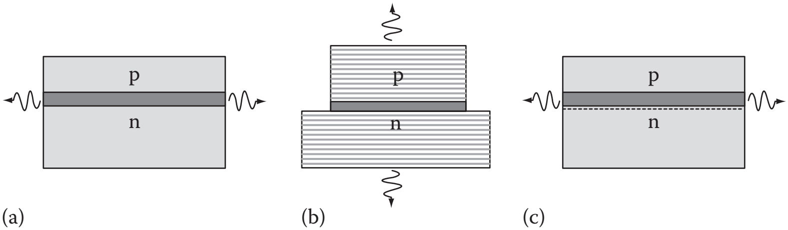

Figure 2.19 Optical resonator designs for semiconductor lasers: (a) Fabry–Perot laser, (b) VCSEL, and (c) DFB laser.

002x019.eps

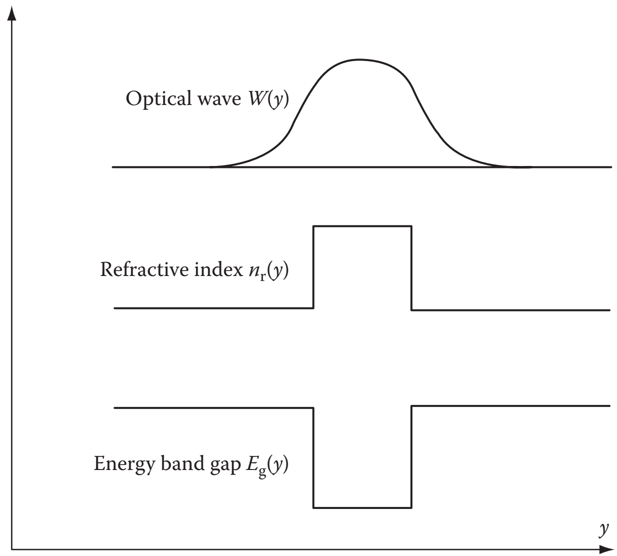

Figure 2.20 Vertical profile of band gap, refractive index, and optical wave within a planar symmetric heterostructure.

002x020.eps

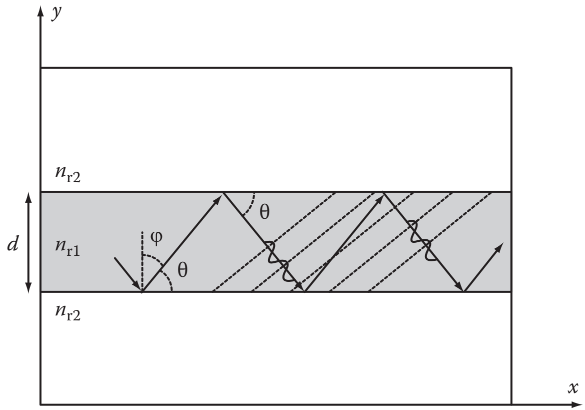

Figure 2.21 Light propagation in a planar waveguide. The dashed lines indicate constructive interference of reflected waves.

002x021.eps

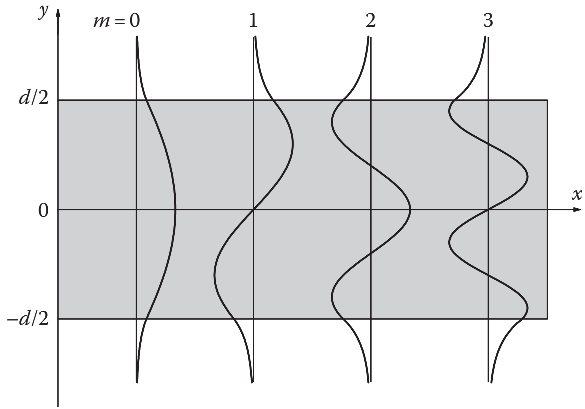

Figure 2.22 Transverse optical field profiles $W_m(y)$ for waveguide mode number m.

002x022.eps

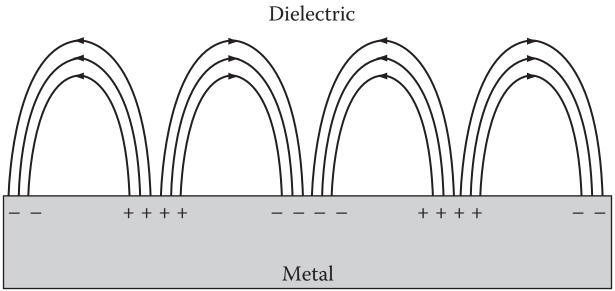

Figure 2.23 Surface plasmons: interaction of electrons and optical waves at a metal/dielectric interface.

002x023.eps

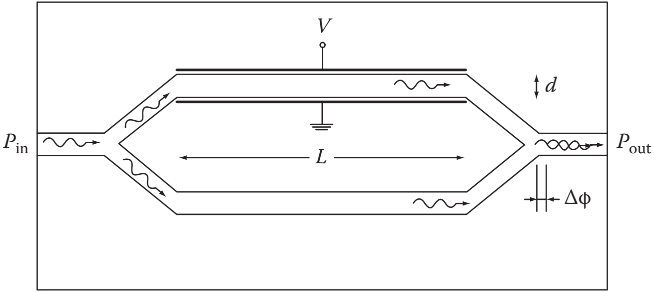

Figure 2.24 Mach–Zehnder modulator.

0c2x024.eps

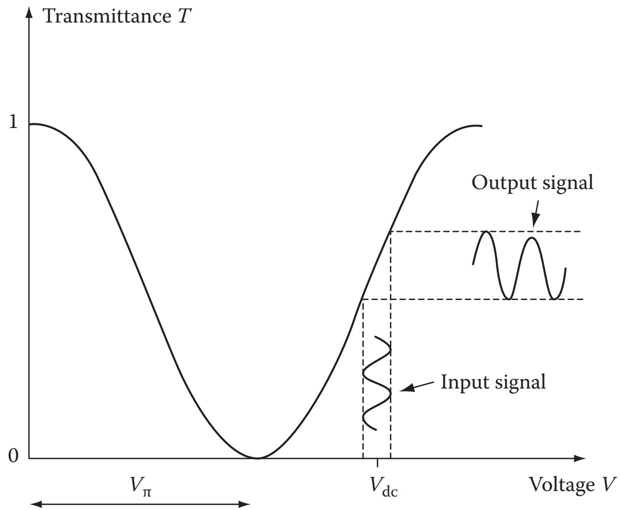

Figure 2.25 Modulator transmittance function $T(V)$.

002x025.eps

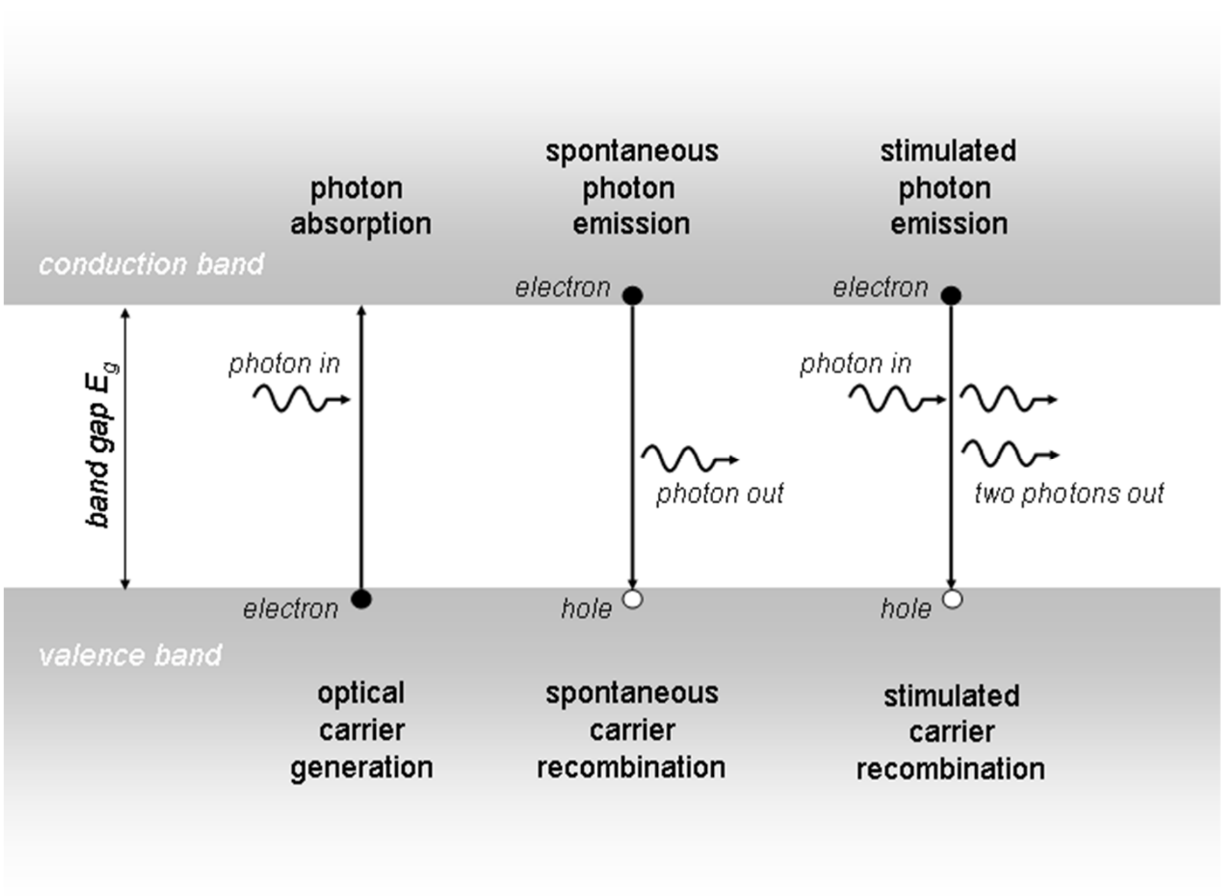

Figure 2.1 Illustration of key processes in optoelectronic devices.

CRC Press, 2008. ISBN-10: 0849392845

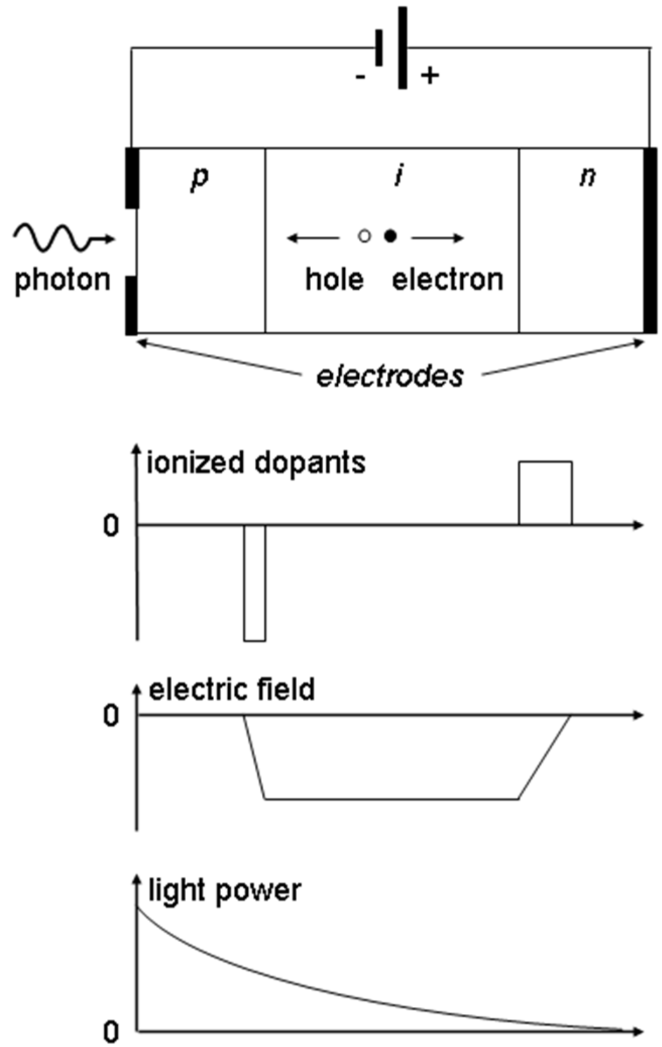

Figure 2.2 Schematic structure and internal physics of *pin* photodiodes.

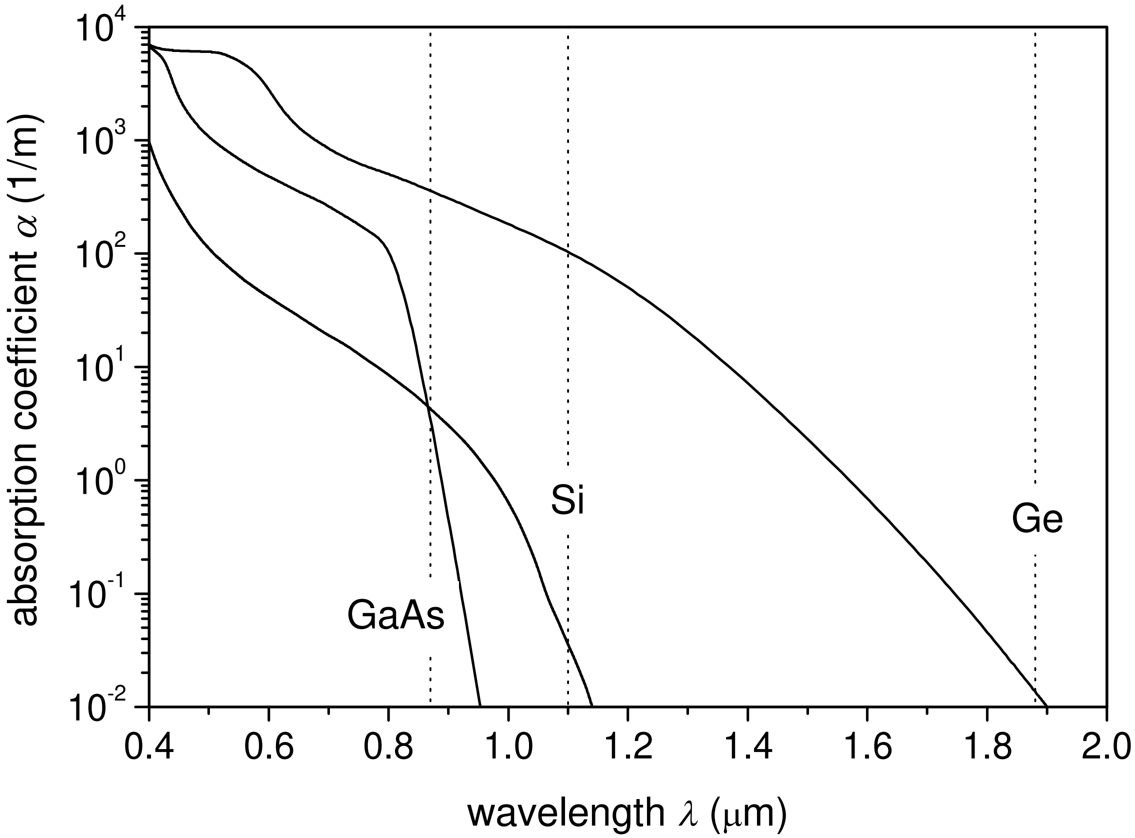

Figure 2.3 Optical absorption constants of GaAs, Si, and Ge as function of light wavelength. The dotted lines indicate the band gap wavelength.

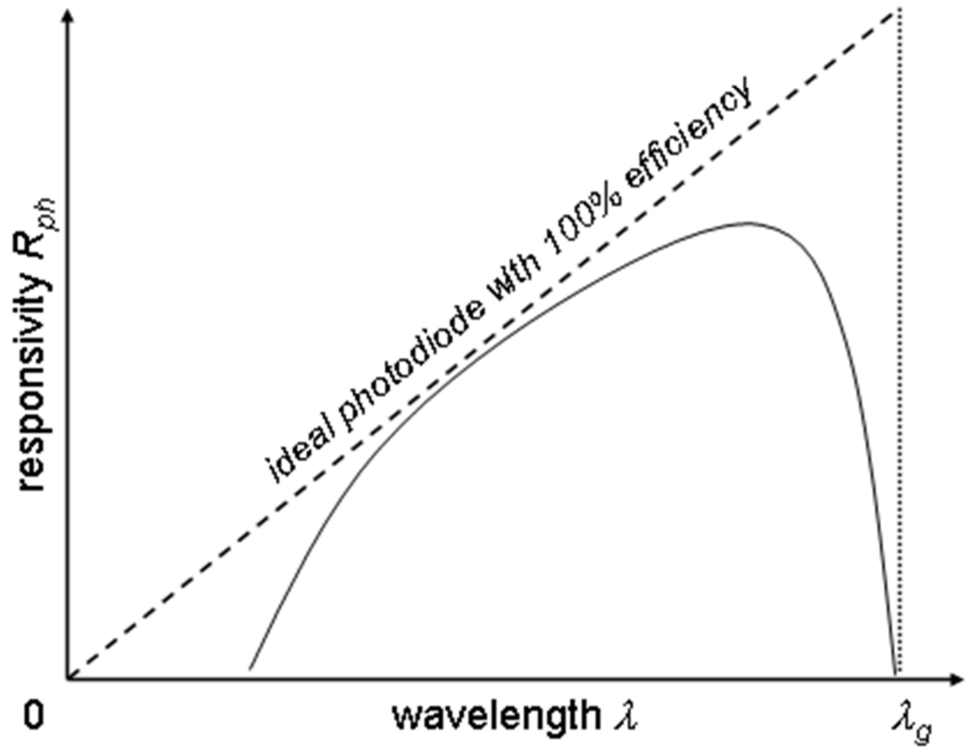

Figure 2.4 Schematic responsivity spectrum of photodiodes.

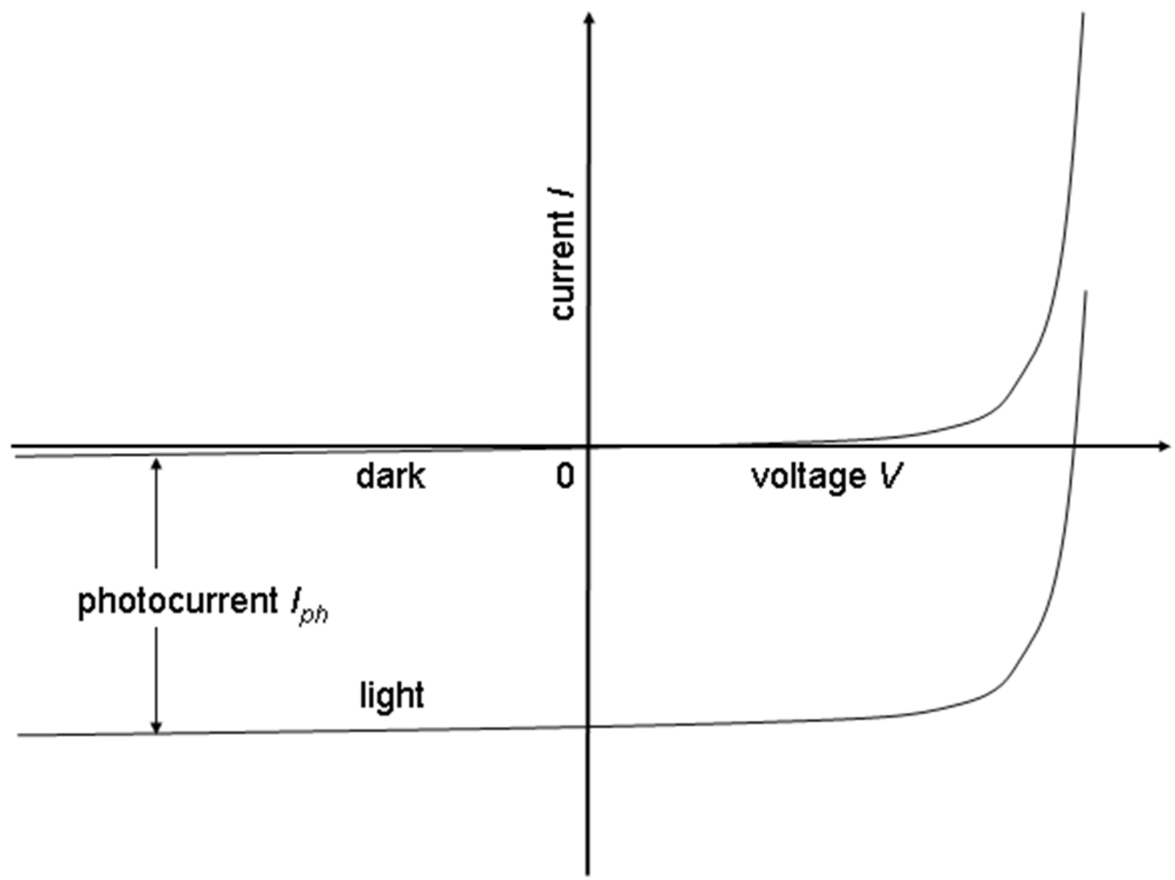

Figure 2.5 Current-voltage characteristic for a photodiode with and without illumination.

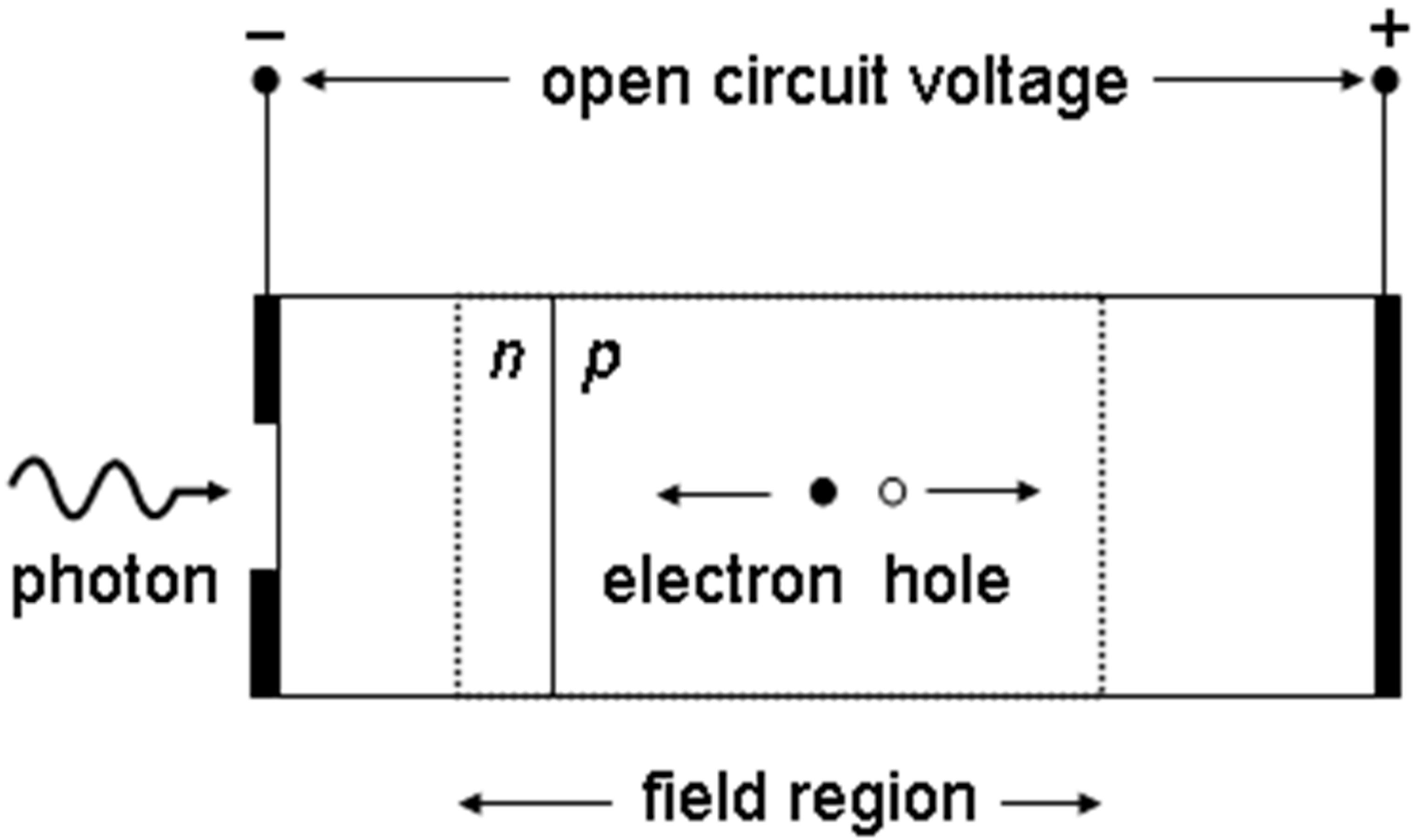

Figure 2.6 Solar cell.

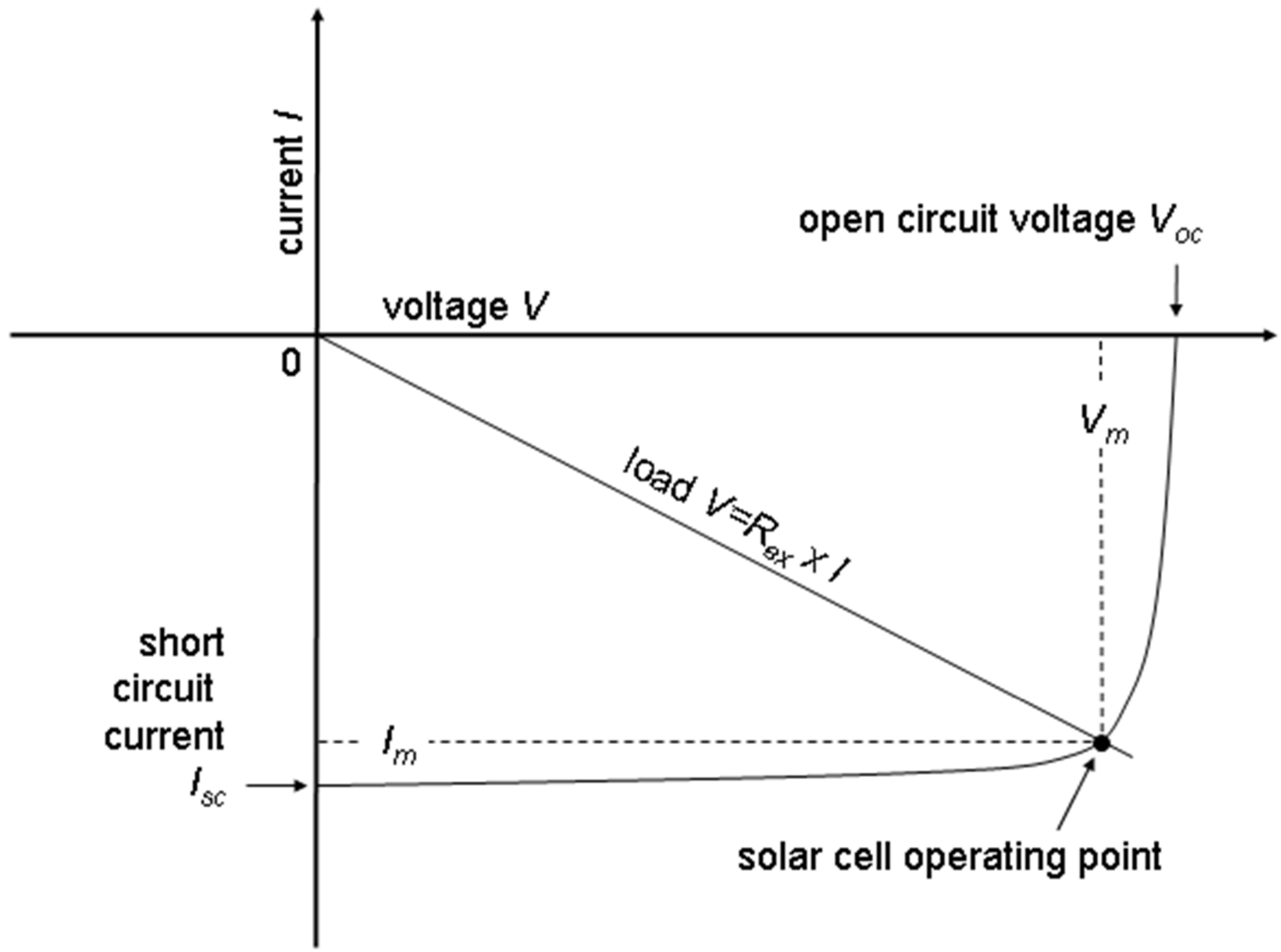

Figure 2.7 Solar cell current-voltage characteristic and parameters.

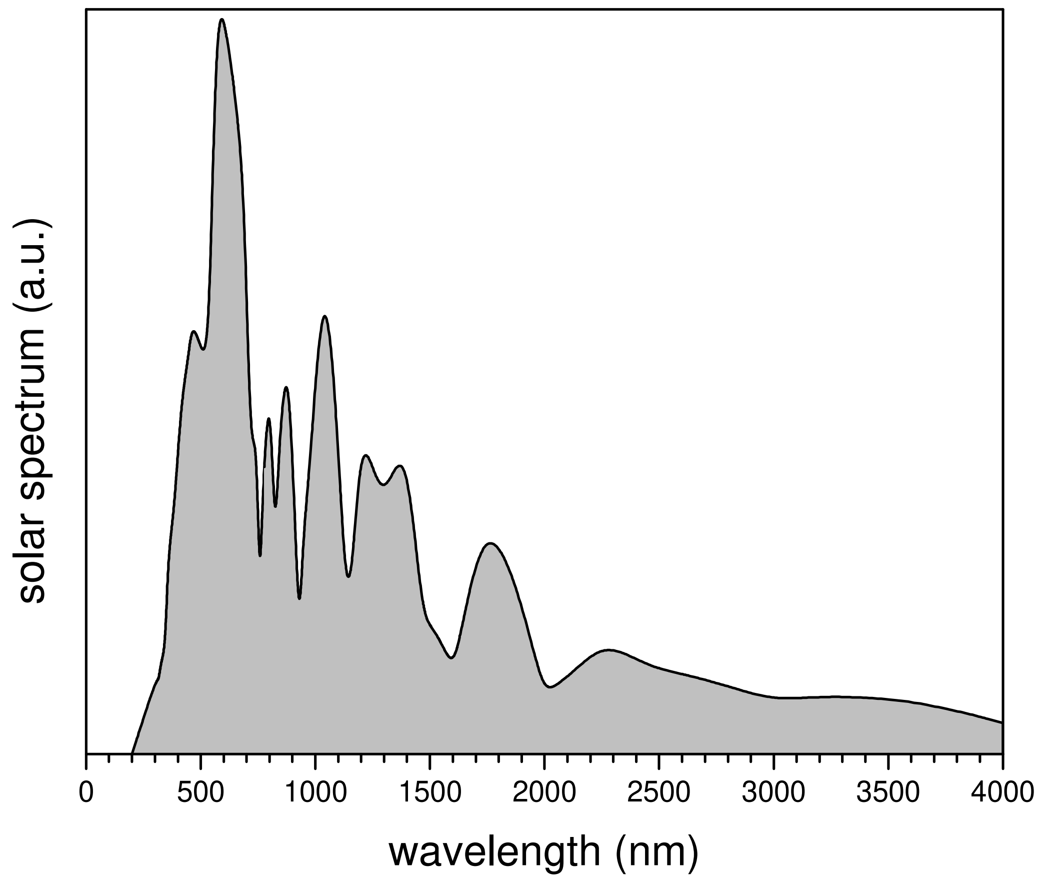

Figure 2.8 Solar spectrum.

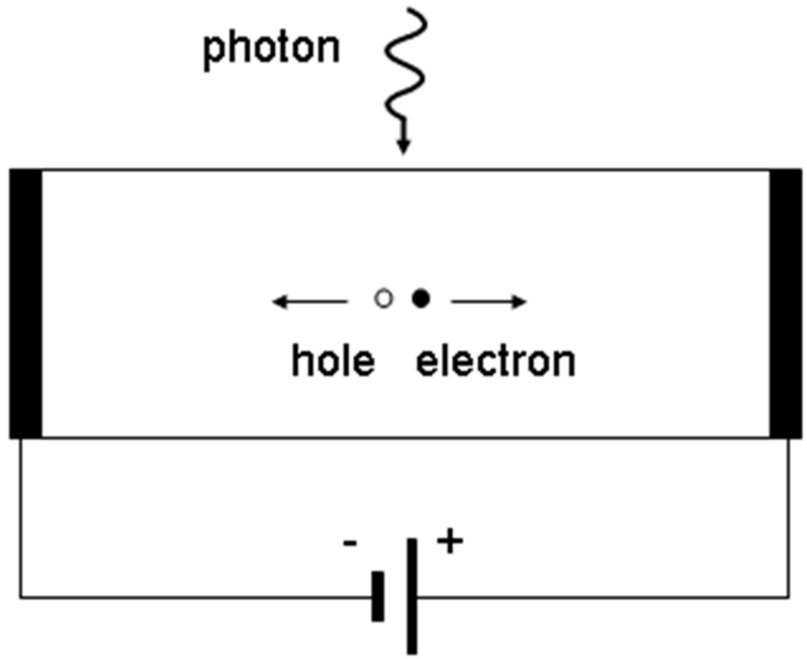

Figure 2.9 Photoconductor.

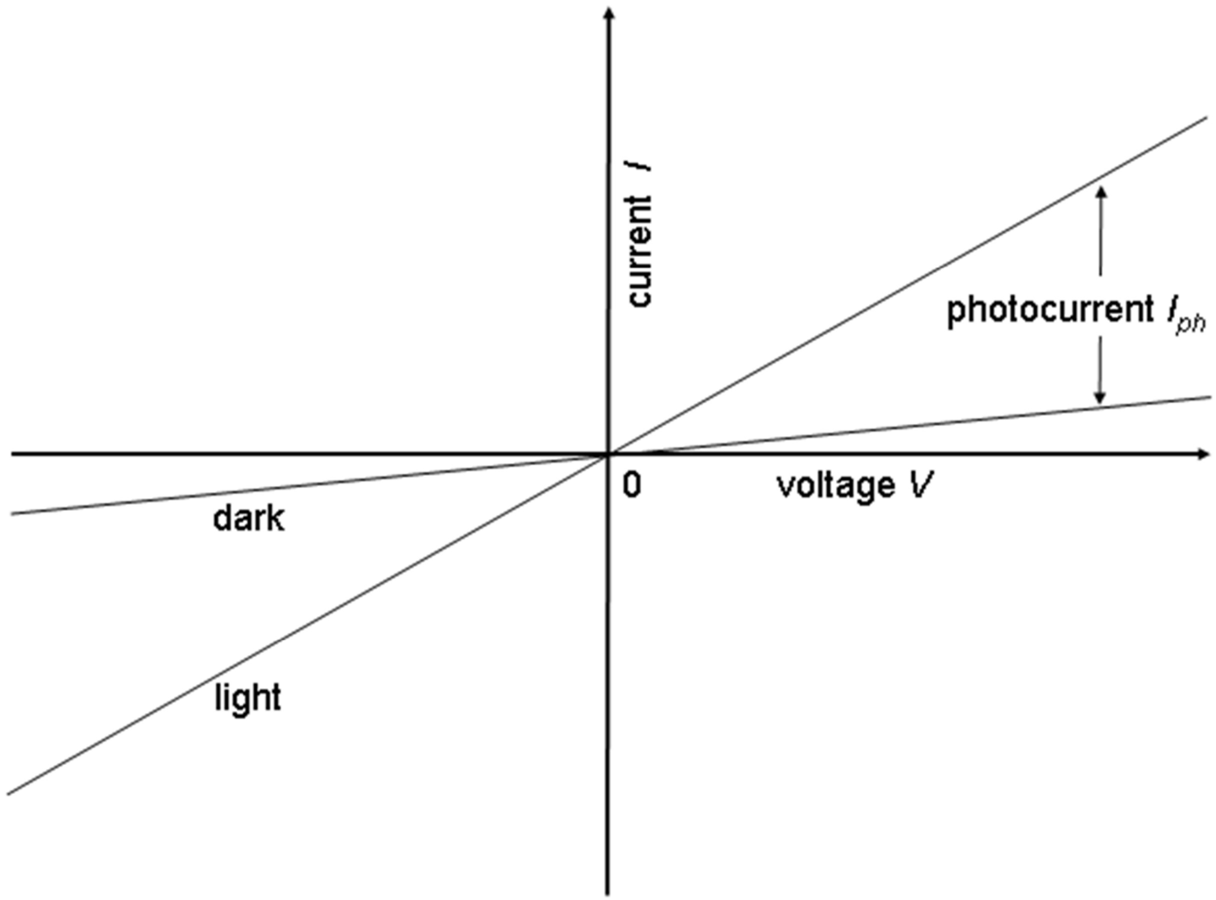

Figure 2.10 Current-voltage characteristic for a photoconductor with and without illumination.

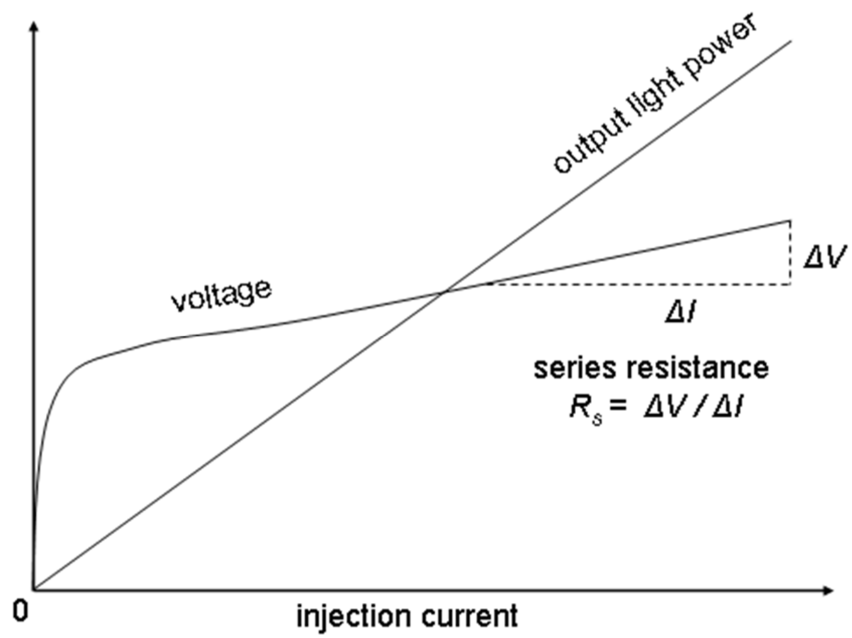

Figure 2.11 Typical LED characteristics: light vs. current (*LI*) and voltage vs. current (*IV*).

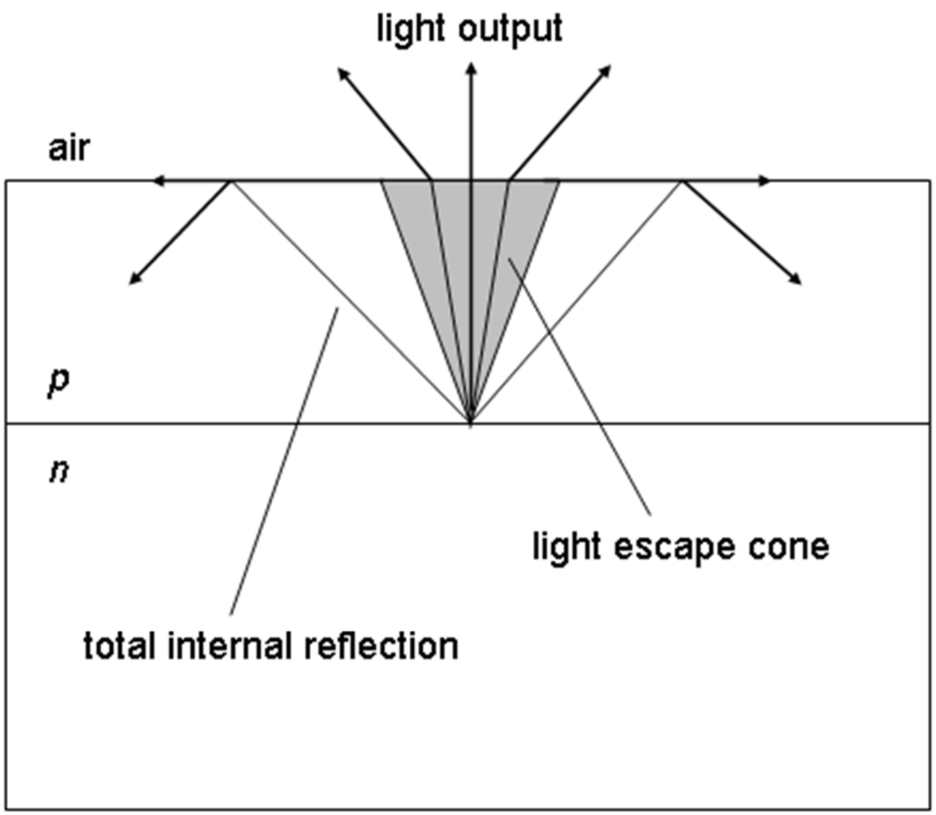

Figure 2.12 Illustration of light propagation in a simple LED structure.

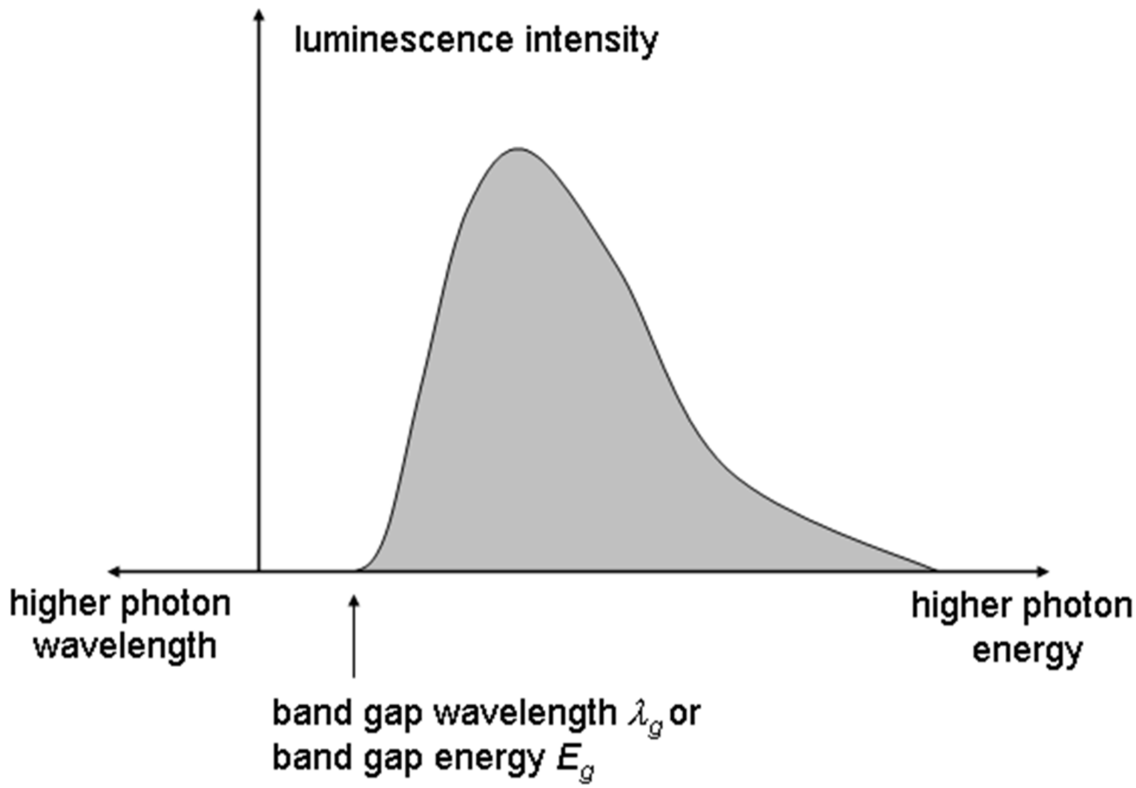

Figure 2.13 Schematic LED emission spectrum.

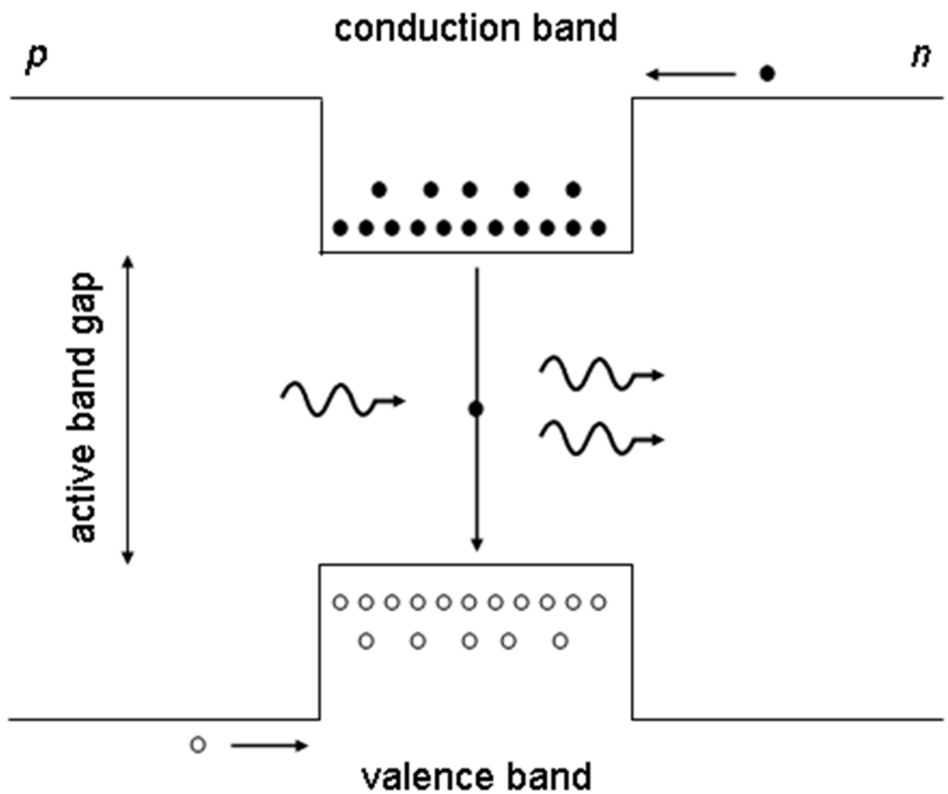

Figure 2.14 Energy band diagram of a *pin*-heterojunction illustrating stimulated photon emission at forward bias.

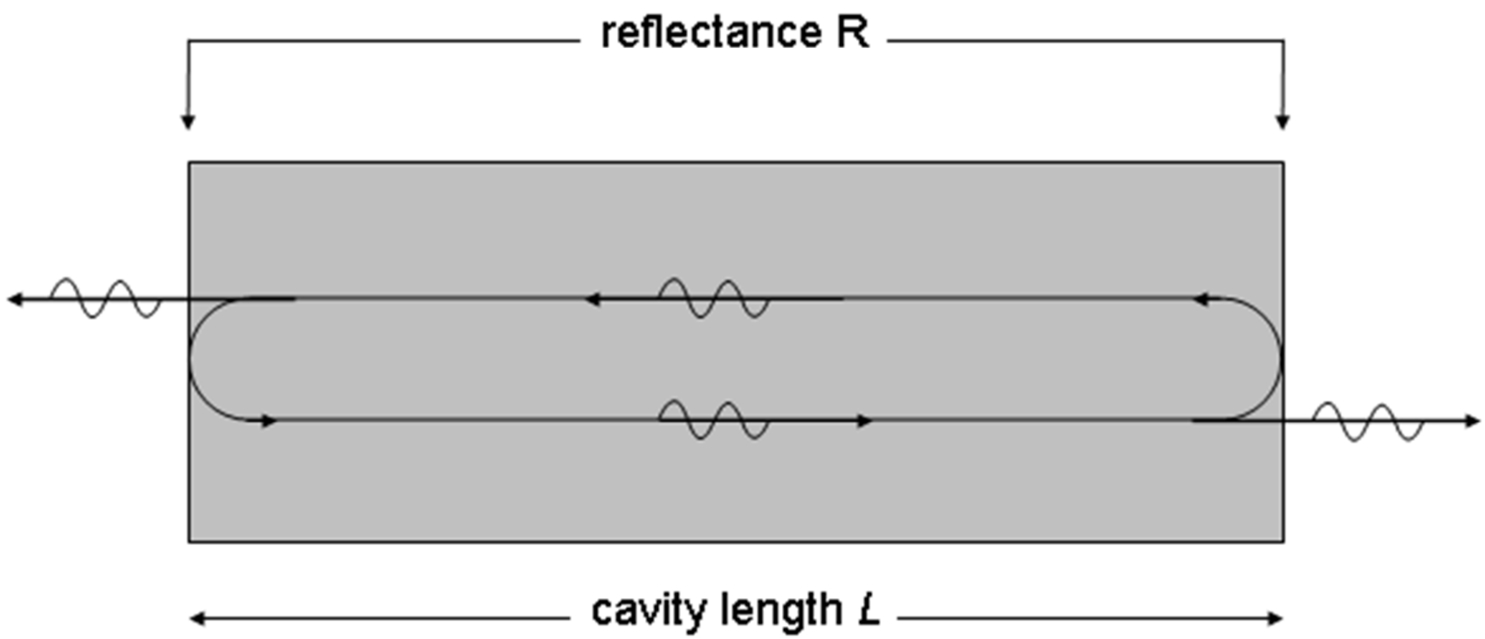

Figure 2.15 Optical feedback in a Fabry-Perot laser.

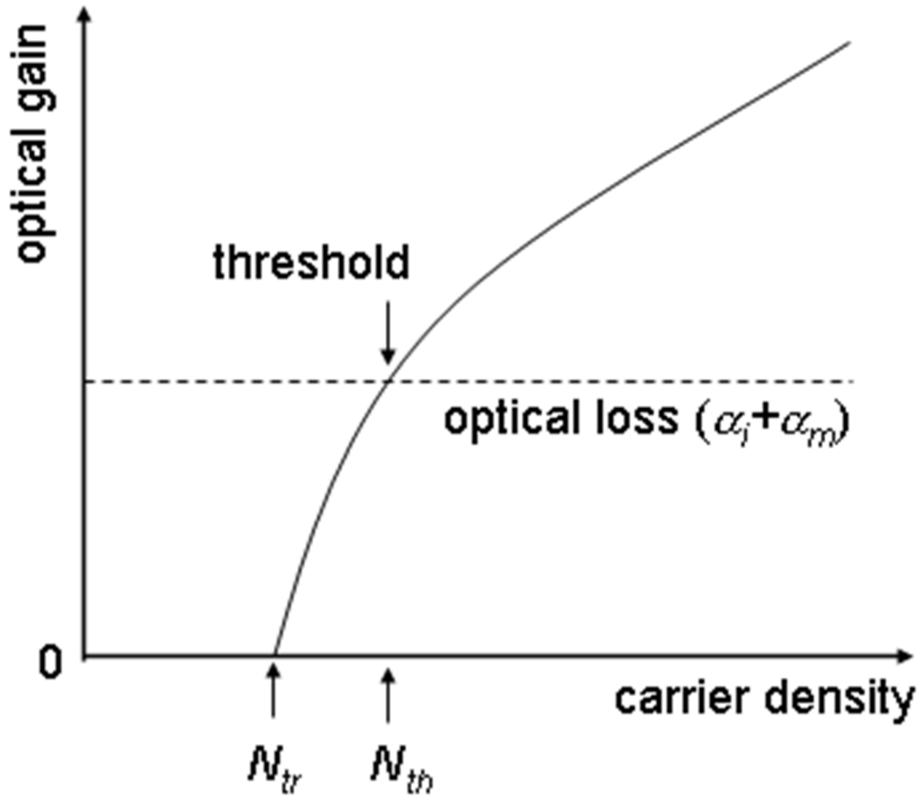

Figure 2.16 Gain versus carrier density *g(N)* with transparency density *Ntr* and threshold density *Nth.*

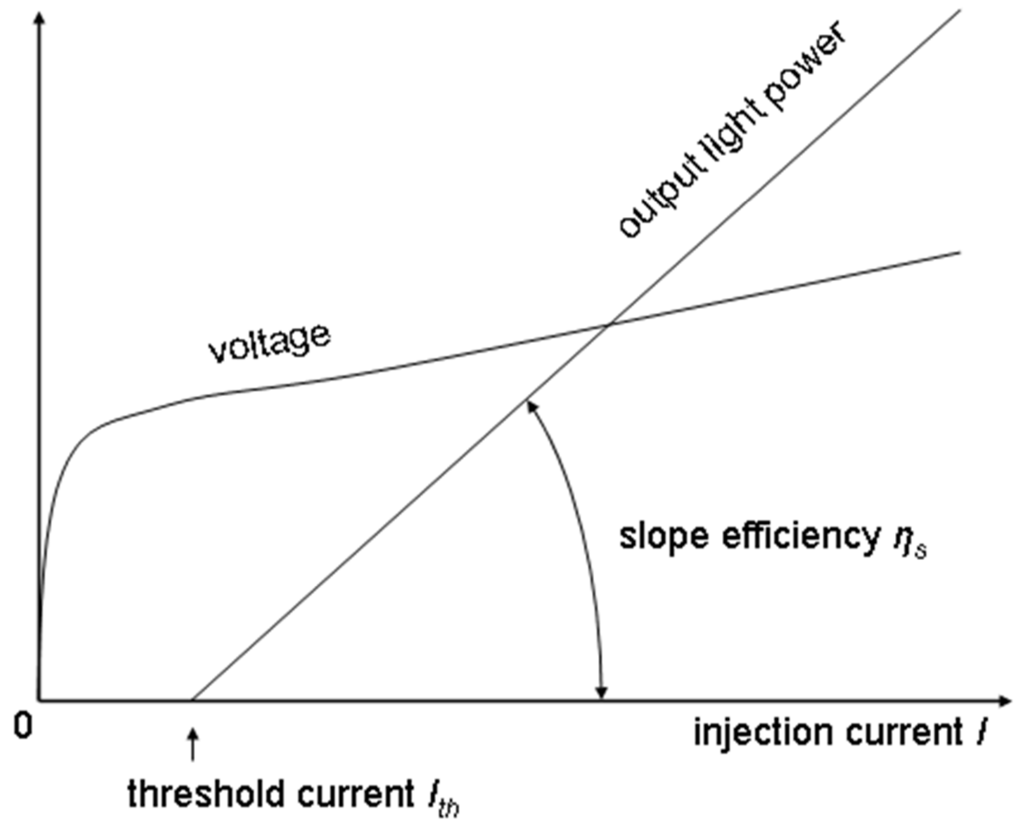

Figure 2.17 Laser characteristics: light power vs. current (LI) and voltage vs. current (IV).

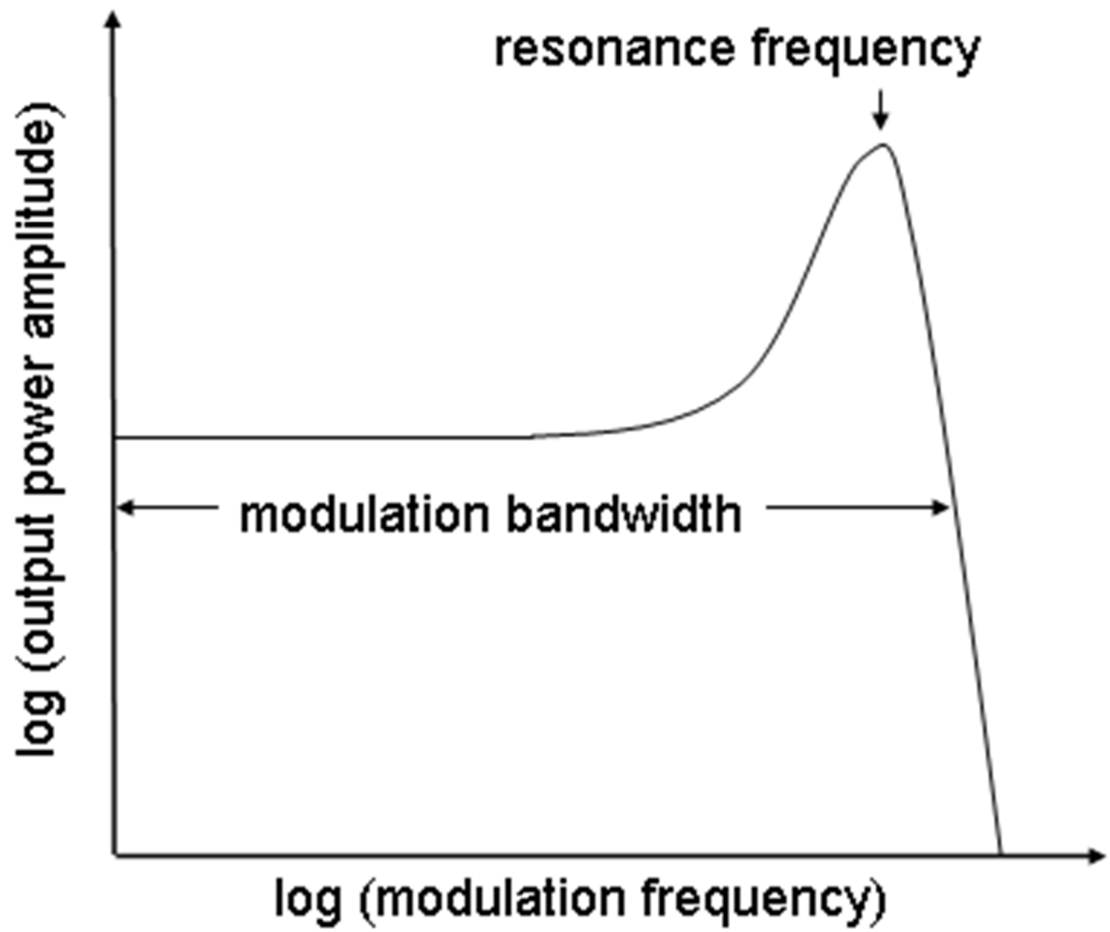

Figure 2.18 Analog modulation characteristic of a laser.

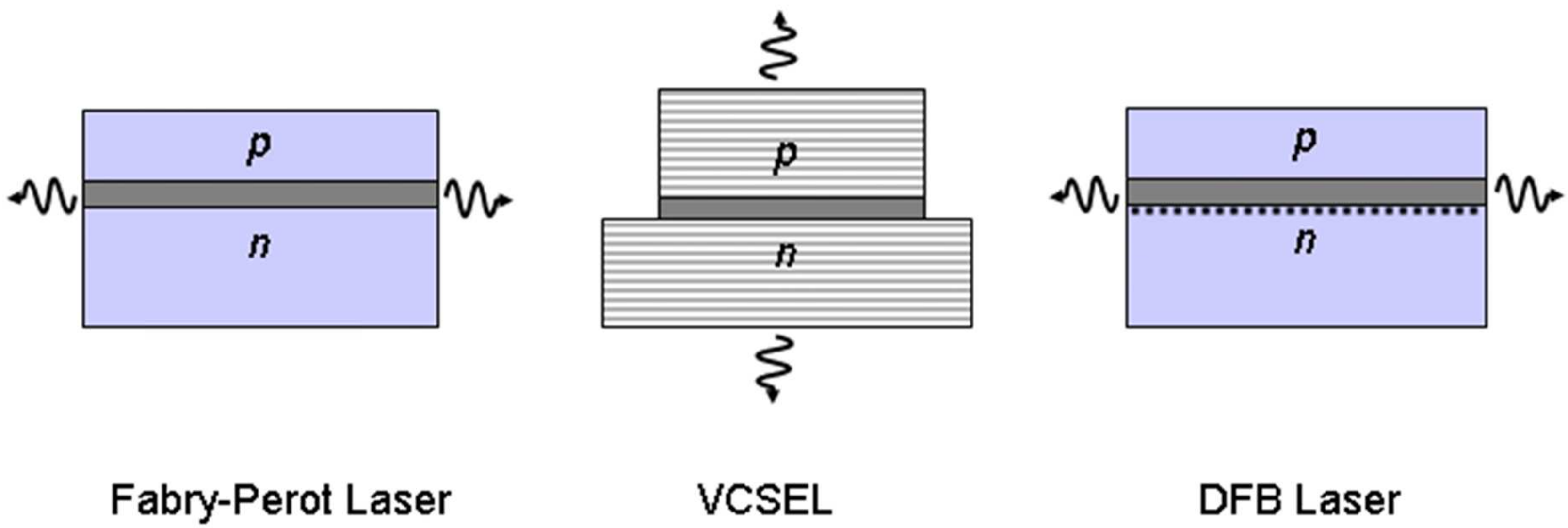

Figure 2.19 Optical resonator designs for semiconductor lasers.

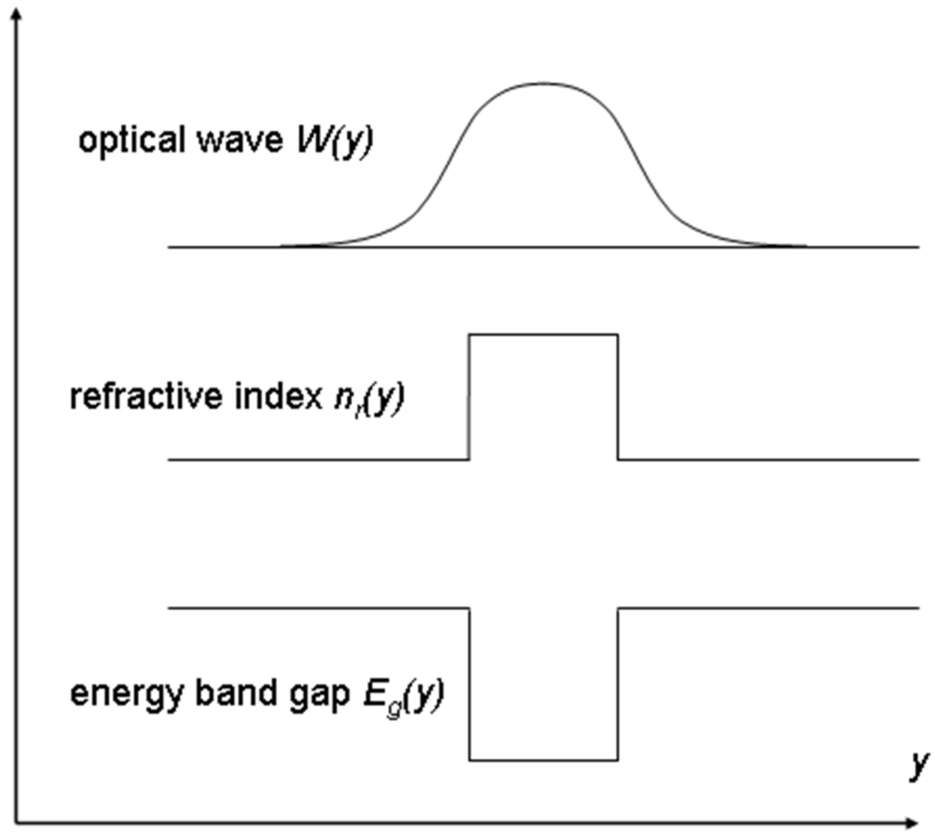

Figure 2.20 Vertical profile of band gap, refractive index, and optical wave within a planar symmetric heterostructure.

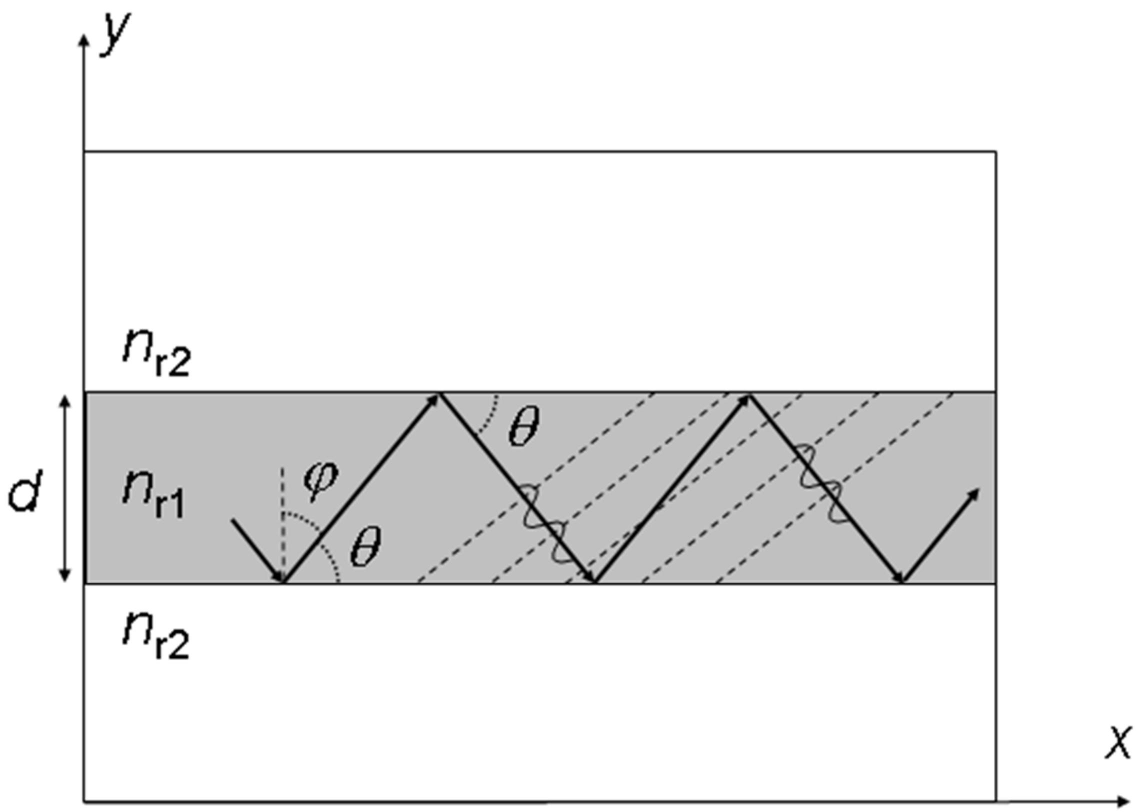

Figure 2.21 Light propagation in a planar waveguide. The dashed lines indicate constructive interference of reflected waves.

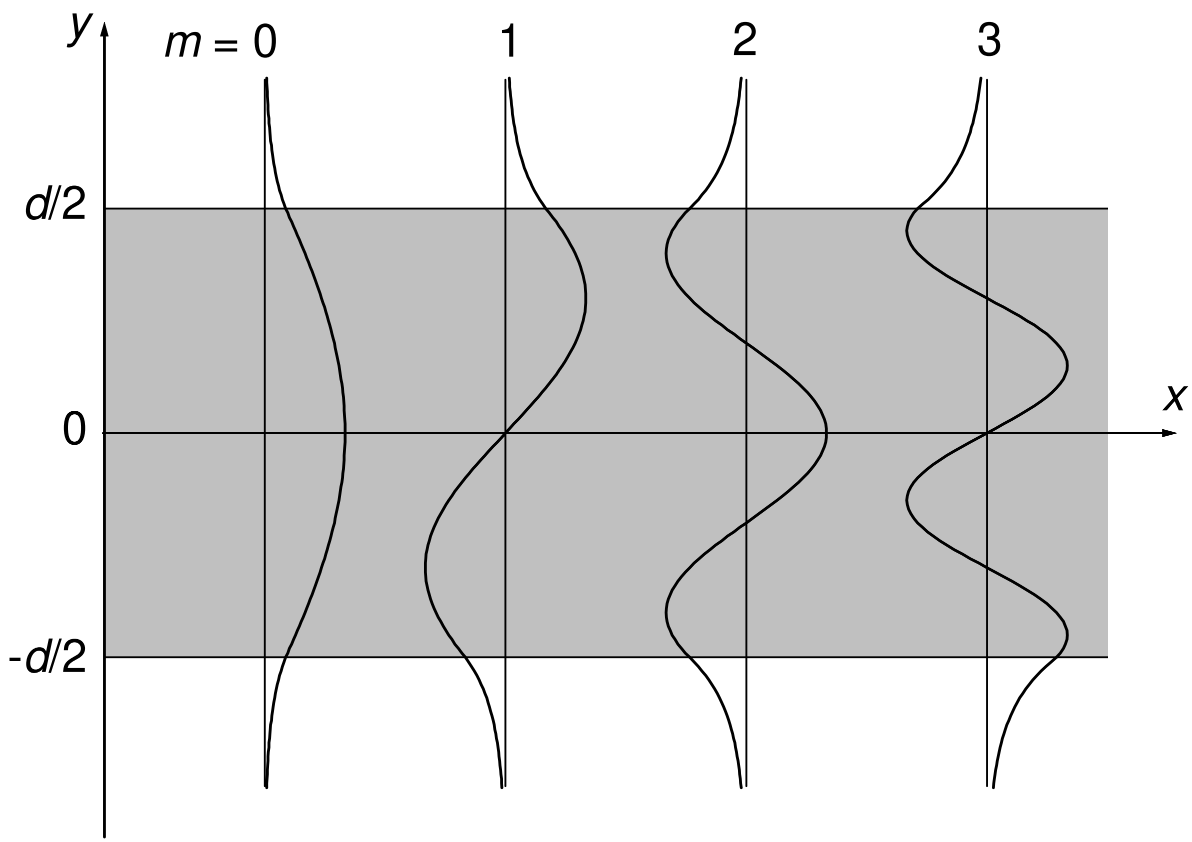

Figure 2.22 Transverse optical field profiles *Wm(y)* for waveguide mode number *m*.

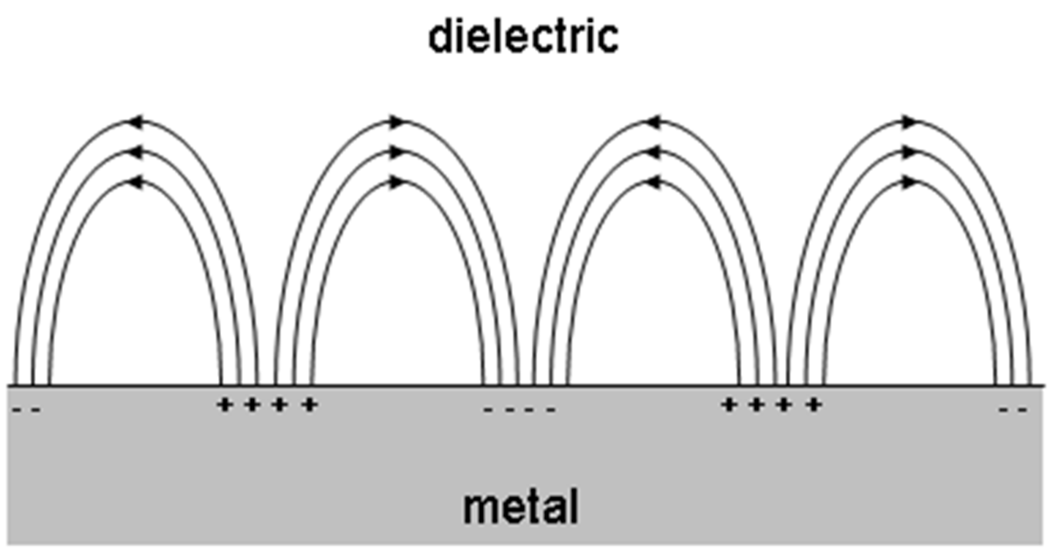

Figure 2.23 Surface plasmons: interaction of electrons and optical waves at a metal / dielectric interface.

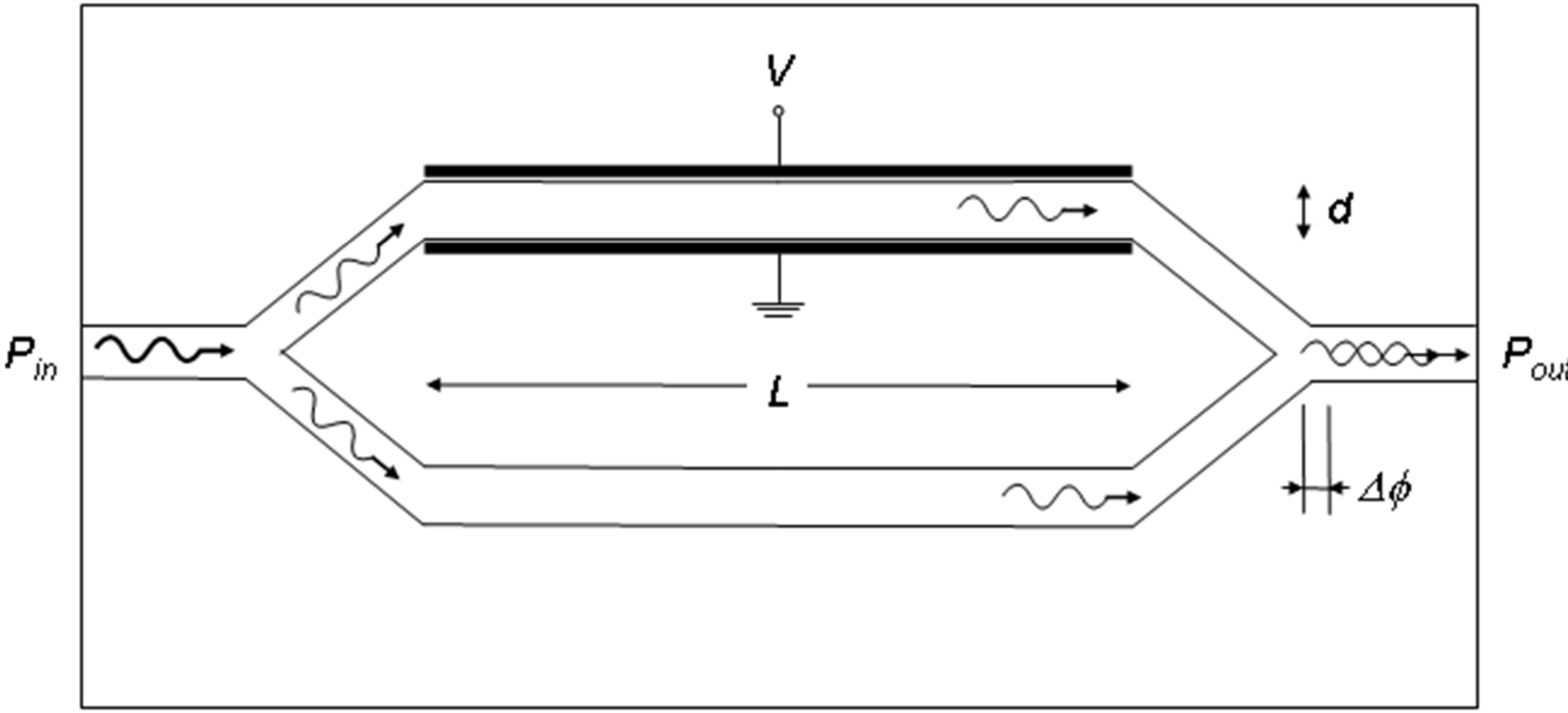

Figure 2.24 Mach-Zehnder Modulator.

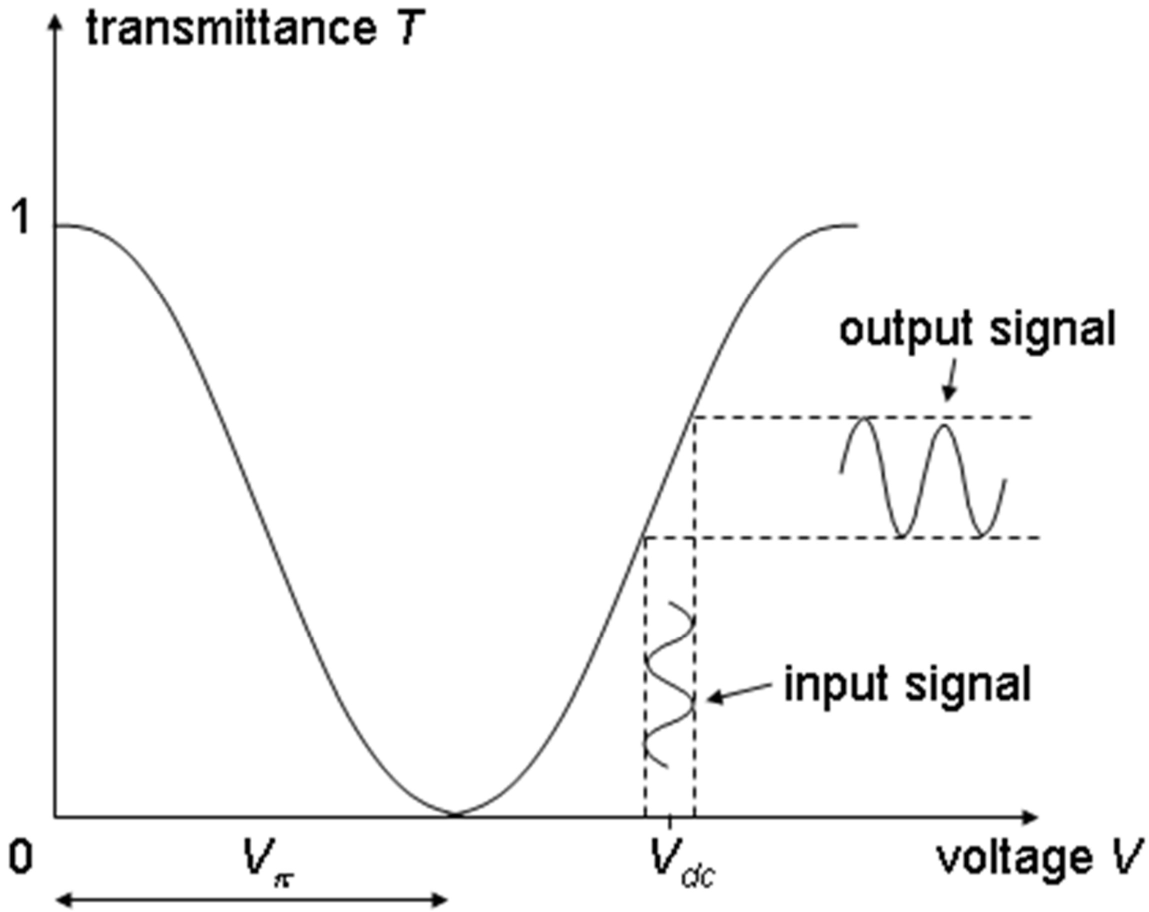

Figure 2.25 Modulator transmittance function *T(V).*